# Modeling the Aliso Canyon underground gas storage well blowout and kill operations using the coupled well-reservoir simulator T2Well

Lehua Pan [*], Curtis M. Oldenburg, Barry M. Freifeld, Preston D. Jordan

*Energy Geosciences Division, Lawrence Berkeley National Laboratory, Berkeley, CA 94720, USA*

## ABSTRACT

A blowout of the Sesnon Standard-25 well (SS-25; API 03700776) at the Aliso Canyon Underground Gas Storage Facility, first observed on October 23, 2015, eventually resulted in emission of nearly 100,000 tonnes of natural gas (mostly methane) to the atmosphere. Several thousand people were displaced from their homes as the blowout spanned 111 days. Seven attempts to gain pressure control and stop the gas flow by injection of heavy kill fluids through the wellhead failed, a process referred to as a "top kill." Introduction of drilling mud when a relief well milled through the casing of SS-25 at a depth of ~8 400 ft ("bottom kill") succeeded in halting the gas flow on February 11, 2016. We carried out coupled well-reservoir numerical modeling using T2Well to assess why the top kills failed to control the blowout. T2Well couples a reservoir simulation in which porous media flow is described using Darcy's law with a discretized wellbore in which the Navier-Stokes momentum equation implemented via a drift-flux model (Shi et al., 2005) is used to describe multi-phase fluid transport to allow detailed process modeling of well blowouts and kill attempts. Modeling reveals the critical importance of well geometry in controlling flow dynamics and the corresponding success or failure of the kill attempts. Geometry plays a role in controlling where fluids can flow, e.g., when gas flow prevents liquid flow from entering the tubing from the annulus, but geometry also provides the opportunity for dead end regions to accumulate stagnant gas and liquid that can also affect kill attempts. Simulations show that follow-up fluid injections after the main kill attempts likely would have been effective to ensure that gas leakage remains stopped. T2Well is capable of simulating well kills and understanding the mechanisms behind well control failures and successes.

## 1. Introduction

A subsurface blowout of the Sesnon Standard-25 (SS-25; API 03700776) well at the Aliso Canyon underground gas storage (UGS) facility, first observed to have ruptured to the ground surface on 23 October 2015, resulted in about 100,000 tonnes of methane and several thousand tonnes of ethane emitted to the atmosphere (Conley et al., 2016; California Air Resources Board, 2016). Several thousand people were displaced from their homes as emitted gases and fumes (e.g., mercaptan odorant) went on for 111 days. Seven attempts failed to stop the flow by gaining pressure control through the injection of dense fluids through the wellhead, so-called top-kill attempts. Introduction of drilling mud when a relief well milled through the SS-25 casing at reservoir depth (~8 400 ft) finally killed the gas leak on February 11, 2016, a method known as a bottom kill. .

Starting in late 2015, our team began numerical modeling of the SS-25 well and the ongoing kill attempts with the goal of understanding why

the attempts were failing and to recommend how the kill attempts could be designed to be effective. Although our team did not have direct experience with UGS well modeling prior to October 2015, we were able to utilize existing simulation capabilities developed over many years and build on long experience in numerical reservoir simulation of two-phase fluid flow. Specifically, we developed coupled well-reservoir simulation capabilities several years ago for application in the area of geologic carbon sequestration where there is a need for modeling carbon dioxide well injection and blowout scenarios for risk assessment (Pan et al., 2011b). Our approach to simulating two-phase coupled well-reservoir systems was to add a well-flow (pipe-flow) modeling capability based on implementing the Navier-Stokes momentum equation via a drift-flux model (DFM, Shi et al., 2005) to LBNL's reservoir simulator TOUGH2 (Pruess et al., 1999, 2011) to create T2Well (Pan et al., 2011c; Pan and Oldenburg, 2014). The integral finite difference method grids used in the TOUGH codes allow modeling of complicated geometries, which were needed to capture flow-path complexities in the SS-25 well
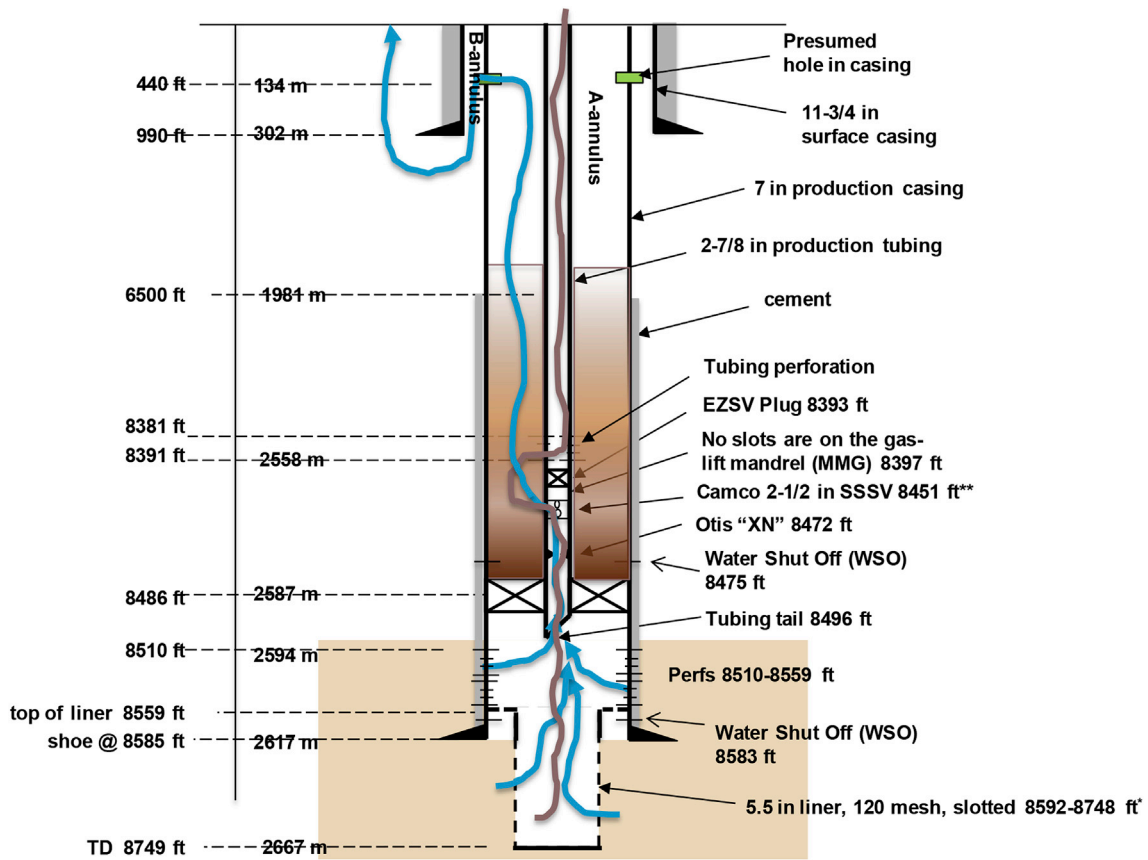
---

**Fig. 1.** A sketch of the SS-25 well (not to scale) and possible flow paths of gas leakage (blue) and kill fluid (brown). * This is believed to be actually 120 Gauge (0.120 inch). ** This is actually the remnants of an SSSV (subsurface safety valve). All that remains are slots between tubing and annulus. Although the exact origin of these slots is uncertain, it is possible they are part of an SSV (sliding sleeve valve) that has been removed and therefore these slots will be called SSV slots in this paper. (For interpretation of the references to colour in this figure legend, the reader is referred to the web version of this article.)

**Table 1**
Governing equations solved in T2Well (see Nomenclature for definition of symbols).

| Description | | Equation |
|---|---|---|
| Conservation of mass and energy | | $\frac{d}{dt}\int_{V_n} M^k dV_n = \int_{\Gamma_n} \mathbf{F}^K \cdot \mathbf{n} d\Gamma_n + \int_{V_n} q^K dV_n$ |
| Mass accumulation | | $M^\kappa = \phi \sum_\beta S_\beta \rho_\beta X_\beta^\kappa$, for each mass component |
| Mass flux | | $\mathbf{F}^\kappa = \sum_\beta X_\beta^\kappa \rho_\beta \mathbf{u}_\beta$, for each mass component |
| Porous media | Energy flux | $\mathbf{F}^\kappa = -\lambda \nabla T + \sum_\beta h_\beta \rho_\beta \mathbf{u}_\beta$ |
| | Energy accumulation | $M^\kappa = (1-\varphi)\rho_R C_R T + \varphi \sum_\beta \rho_\beta S_\beta U_\beta$ |
| | Phase velocity | $\mathbf{u}_\beta = -k\frac{k_{r\beta}}{\mu_\beta}(\nabla P_\beta - \rho_\beta \mathbf{g})$   Darcy's Law |
| Wellbore | Energy flux | $F^\kappa = -\lambda \frac{\partial T}{\partial z} - \frac{1}{A}\sum_\beta \left[A\rho_\beta S_\beta u_\beta \left(h_\beta + \frac{u_\beta^2}{2} + gz\cos\theta\right)\right] + q'$ |
| | Energy accumulation | $M^\kappa = \sum_\beta \rho_\beta S_\beta \left(U_\beta \frac{u_\beta^2}{2} + gz\cos\theta\right)$ |
| | Phase velocity | $u_G = C_0 \frac{\rho_m}{\rho_m^*}u_m + \frac{\rho_L}{\rho_m^*}u_d$ |
| | | $u_L = \frac{(1-S_G C_0)\rho_m}{(1-S_G)\rho_m^*}u_m - \frac{S_G \rho_G}{(1-S_G)\rho_m^*}u_d$   Drift − Flux − Model |

described below.

Despite the original target application being geologic carbon sequestration, T2Well is a general coupled well-reservoir simulator that can be used for a variety of applications. For example, we modified the code slightly in 2010 to simulate the Macondo well oil and gas blowout in the Gulf of Mexico in response to the urgent need for flow-rate estimation (Oldenburg et al., 2012). T2Well is also used in geothermal reservoir modeling studies (e.g., Pan et al., 2015; Vasini, 2016) and aquifer-based compressed air energy storage studies (Oldenburg and Pan, 2013a; b; Guo et al., 2016). Applications of T2Well in various areas have confirmed
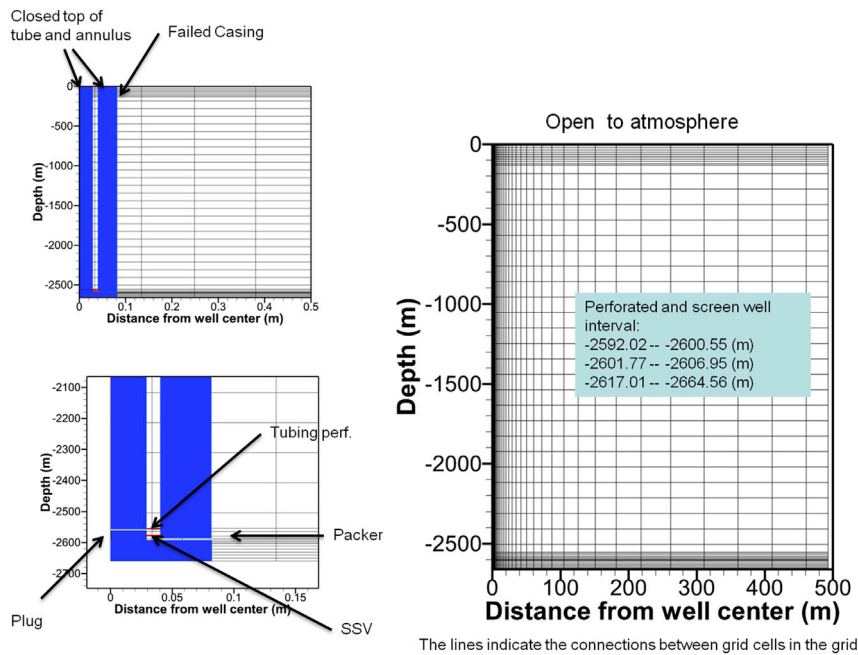
**Fig. 2.** Radially symmetric grid for modeling blowout and top kills of the SS-25 well system showing the large range in length scales needed to model integrated well-reservoir systems. The left-hand side, upper figure shows the refined mesh for the well (tubing, tubing wall, and annulus) and surrounding formation. The left-hand side, lower figure shows details of the tubing plug (white gap), tubing perforations (red line), the packer (white gap), and the SSV slots (red line) in the mesh. Void space inside the well (tubing or annulus) is marked by the blue color. The right-hand side figure shows the entire mesh showing the large radius of the full system. The lateral resolution of the grid starts at 5 cm near well and then grows at a rate of 1.2 × per block until the domain size reaches 50 m. (For interpretation of the references to colour in this figure legend, the reader is referred to the web version of this article.)

**Table 2**
Formations properties.

| Formation | Depth (m) | Porosity | Horizontal permeability ($10^{-15}$ m²) | Vertical permeability ($10^{-15}$ m²) | Notes |
|---|---|---|---|---|---|
| 1 | 0.0–129.2 | 0.169 | 8600 | 3000 | Shallow formations |
| 2 | 129.2–135.3 | 0.254 | 10000 | 10000 | |
| 3 | 135.3–2252.7 | 0.288 | 230 | 95 | |
| 4 | 2252.7–2256.4 | 0.139 | 2.4 | 0.083 | Cap rocks |
| 5 | 2256.4–2574.0 | 0.315 | 350 | 0.01 | |
| 6 | 2574.0–2584.7 | 0.283 | 230 | 0.81 | |
| 7 | 2584.8–2592.0 | 0.083 | 0.003 | 0.00001 | |
| 8 | 2592.0–2600.6 | 0.315 | 80 | 2.0 | 1st feed zone |
| 9 | 2600.6–2601.7 | 0.139 | 2.4 | 0.08 | Shale in reservoir |
| 10 | 2601.7–2607.0 | 0.315 | 80 | 2.0 | 2nd feed zone |
| 11 | 2607.0–2617.0 | 0.315 | 2.0 | 0.08 | Shale in reservoir |
| 12 | 2617.0–2655.1 | 0.315 | 80 | 2.0 | 3rd feed zone |

**Table 3**
Wellbore properties.

| Section | Depth (m) | Internal Diameter (m) | External diameter of tube (m) | Wall roughness ($10^{-6}$ m) |
|---|---|---|---|---|
| Tubing | 0–2592 | 0.062 | – | 30 |
| Casing (below packer) | 2592–2607 | 0.1595 | – | 45 |
| Casing (above packer, annulus) | 0–2592 | 0.1595 | 0.073 | 67.5 |
| Screen | 2607–2655 | 0.1236 | – | 45 |

the importance of modeling the coupling between the well and the reservoir, which can limit the supply of fluid to the well. T2Well simulations have also shown the importance of modeling two-phase flow and associated depressurization effects associated with upward flow in the well, which can lead to gas exsolution and gas volume expansion that can interfere with (limit) liquid-phase flow (Oldenburg et al., 2012).

The purpose of this paper is to describe the methods used in T2Well and their applicability to modeling well blowouts, and to present detailed modeling analyses of flow, kill attempts, and kill designs related to the Aliso Canyon SS-25 well blowout. The SS-25 well presented some

particular challenges that demanded novel gridding approaches to capture the complex flow interconnections between the tubing and casing. As we will show, the well configuration prevented standard top-kill approaches from working as planned. Simulations suggest that the main feature that prevented effective top kills was the interconnection between the tubing and the A-annulus (the annulus outside of the tubing and inside of the production casing, Fig. 1) that was utilized for natural gas injection and production. Through our modeling work we demonstrate the profound importance of well geometry on flow blocking, liquid entrainment and expulsion by gas, and creation of stagnant zones in the
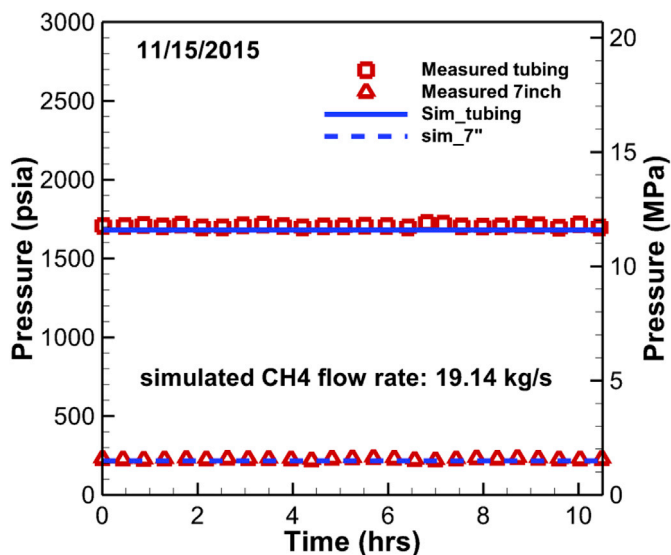
**Fig. 3.** Simulated and measured tubing and production (7″ or 7-in) casing pressure under blowout conditions before the 11/15/2015 top-kill operation with manual calibration of the production casing hole diameter and shallow formation permeability.

**Table 4**
Fluid velocity at various locations along the leakage pathway (as marked on Fig. 4).

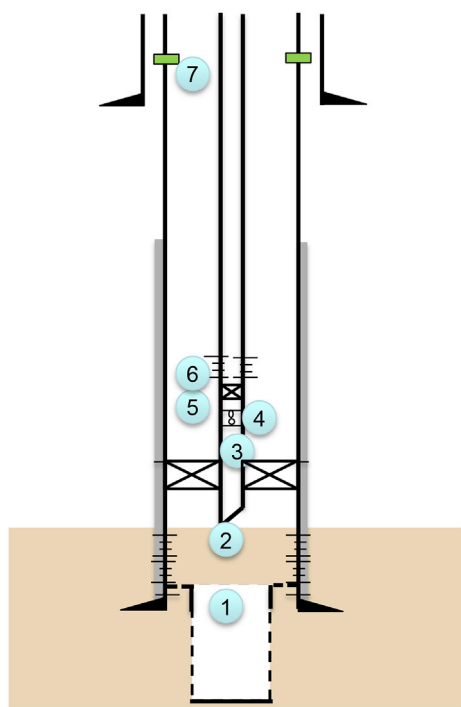| Point | Location | Velocity (m/s) |
|---|---|---|
| 1 | Top of 5.5″ liner | 9.64 |
| 2 | 7″ perforated zone | 6.87 |
| 3 | Tubing below SSV | 70.24 |
| 4 | Through SSV slots | 49.83 |
| 5 | 7″ casing after SSV | 13.90 |
| 6 | 7″ casing below tubing perf. | 13.68 |
| 7 | 7″ casing below leaking point | 120.37 |



**Fig. 4.** Sketch enumerates the various locations along the leakage pathway of the well under blowout conditions at which fluid velocities are reported in Table 4.

**Table 5**
Kill-fluid properties and injection schedules used in the simulations.

| | 242 bbl kill | | 1100 bbl kill | |
|---|---|---|---|---|
| Relative viscosity[a] | 2.4540 | | 1.3886 | |
| Relative density[a] | 1.1834 | | 1.0107 | |
| Schedule | Time (s) | Rate (kg/s) | Time (s) | Rate (kg/s) |
| | 0–600 | 12.83 | 0–600 | 16.29 |
| | 600–2247 | 23.61 | 600–5822 | 32.75 |
| | 2247 | 0.00 | 5822 - | 0.0 |

[a] Relative values are calculated as the ratio to pure water properties at 1 atm and 15.6 °C.

well. The simulations show that consideration of well geometry is critical to the planning and execution of successful well kills during blowout events.
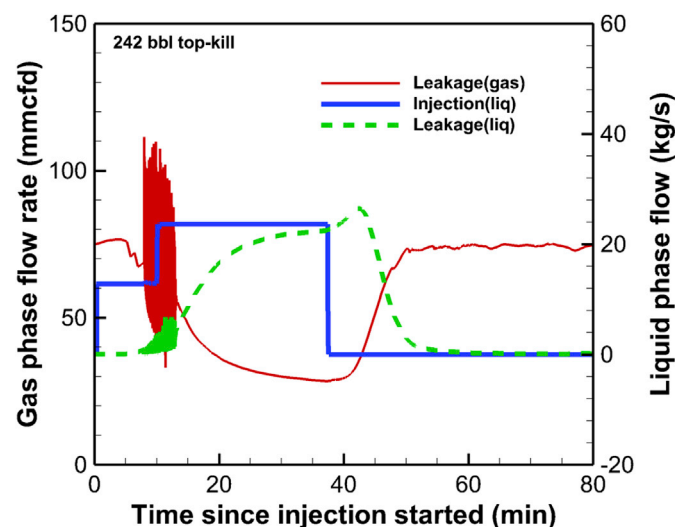


**Fig. 5.** Simulated gas (red line) and liquid (green dashed line) flow through the casing failure plotted along with the injection rate of kill fluid (blue line) during the 242 bbl kill. (For interpretation of the references to colour in this figure legend, the reader is referred to the web version of this article.)



**Fig. 6.** Simulated gas (red line) and liquid (green dashed line) flow rates through the SSV slots from the tubing side to the A-annulus side plotted along with the injection rate of kill fluid (blue line) during the 242 bbl kill. (For interpretation of the references to colour in this figure legend, the reader is referred to the web version of this article.)
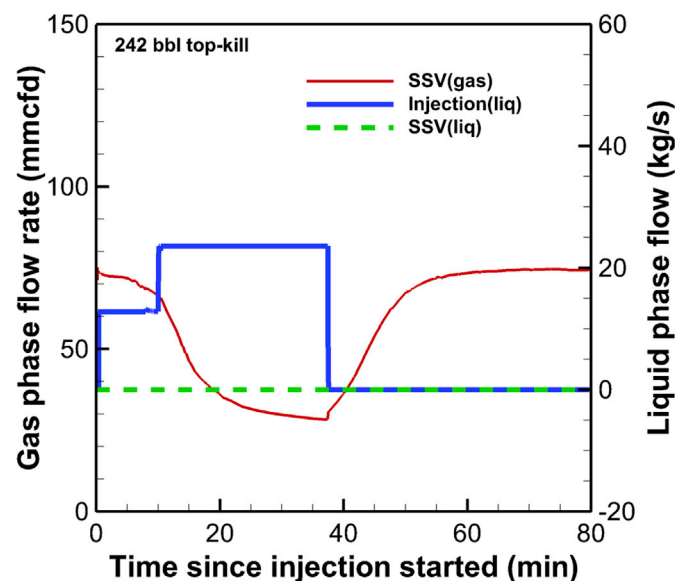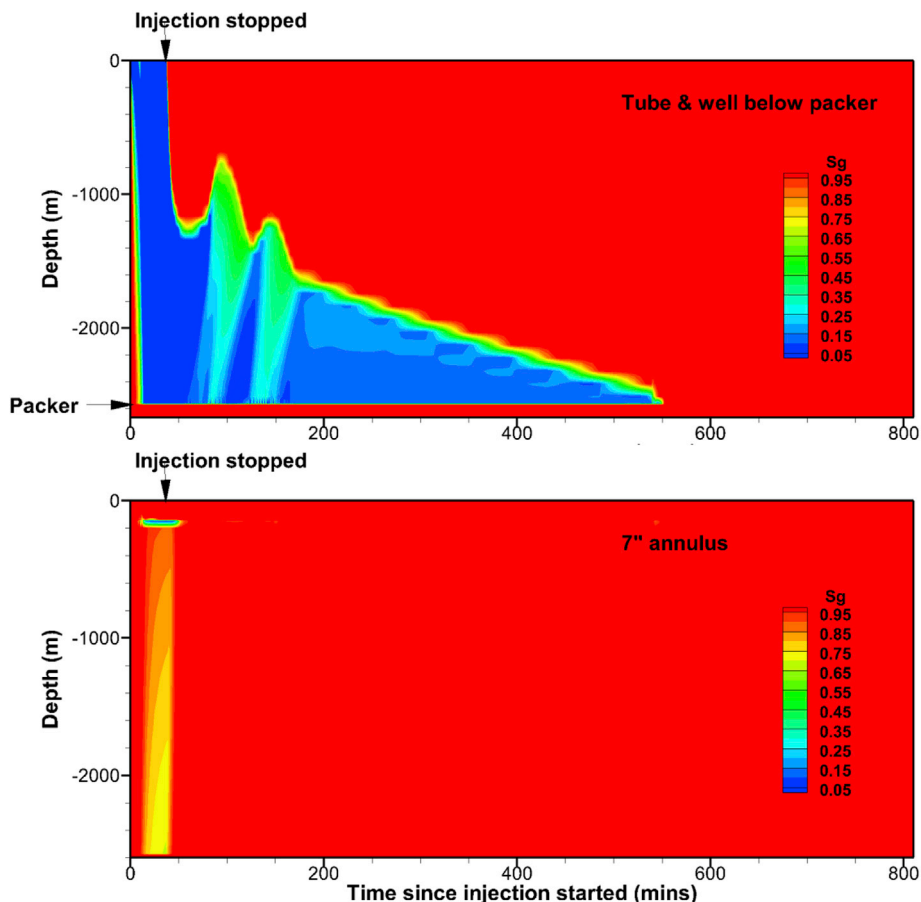
**Fig. 7.** Simulated gas saturation profiles in the tubing and in the well below the packer (upper panel) and 7" (7-in) annulus (lower panel) as a function of time during the 242 bbl kill.

## 2. Methods

### 2.1. Standard well flow simulation

The state-of-the-art simulation codes used by industry for analysis of multiphase well flow, including design of well kills, are based on OLGA, a transient pipe-flow model originally developed for modeling two-phase flow in pipelines (e.g., Bendiksen et al., 1991). OLGA solves two momentum equations, one for the liquid and one for the combination of gas and liquid droplets contained in the gas. Friction factors on the pipe wall are adjusted in OLGA as a function of flow regime. With gravitational terms controlling liquid-gas separation, OLGA can handle stratified flows in horizontal pipes, along with flow in inclined and vertical pipes, which serves to model vertical wells. As such, OLGA has become an industry standard for modeling well kills including dynamic well kills, which are kills based on introducing fluids that increase friction to flow rather than control pressure by building up a dense, static fluid column (e.g., Rygg and Smestad, 1992; Dhulesia and Lopez, 1996; Ravndal, 2011). Although OLGA models flow in the pipe or well with proven accuracy as demonstrated by over 30 years of development and use, OLGA-based models are not fully coupled to the reservoir that supplies the fluid, or in the case of SS-25, the flow is not coupled to the shallow formation into which the blowout was flowing from the well. By fully coupling well flow with flows in the porous media formations connected to the well, T2Well captures the essential interactions between fluid supply and loss related to the well-blowout process as described below. In addition, the flexibility of the integral finite difference grid used in the TOUGH codes upon which T2Well is based allows modeling of complex flow paths and well geometry.

### 2.2. T2Well coupled well-reservoir simulation

T2Well is a numerical simulator for modeling non-isothermal, multiphase, and multicomponent fluid and energy flow in integrated well-reservoir systems (Pan et al., 2011a, 2011c; Pan and Oldenburg, 2014). In T2Well, the flow in the well is described by the two-phase momentum equations whereas the flow in the reservoir is described by multiphase Darcy law (Table 1). By applying the DFM, the two-phase momentum equations are lumped into a momentum equation of the mixture (Eq. (1)), which can be solved for the mixture velocity $u_m$ (Pan et al., 2011a):

$$\frac{\partial}{\partial t}(\rho_m u_m) + \frac{1}{A}\frac{\partial}{\partial z}\left[A\left(\rho_m u_m^2 + \gamma\right)\right] = -\frac{\partial p}{\partial z} - \frac{\Gamma f \rho_m |u_m| u_m}{2A} - \rho_m g \cos\theta \quad (1)$$

In Eq. (1), $t$ is time, $z$ is distance, $A$ is cross sectional area of the flow path, $\gamma$ is a phase-slip term (a complex function of local two-phase flow regime described by DFM), p is pressure, $\Gamma$ is the perimeter of the cross sectional area, $f$ is the friction coefficient (a function of Reynolds number and other geometric parameters), $\rho_m$ is the mixture density, $g$ is gravitational acceleration, and $\theta$ is the inclination angle (symbols are also defined in Nomenclature). The complete methods implemented in T2Well have been fully described elsewhere (Pan et al., 2011c; Pan and Oldenburg, 2014) and will not be duplicated here.

In order to model the flow in a well with complicated geometry such as that in SS-25 (to be described in the next section), we modified the calculation of the effective diameter, which is used to calculate the friction coefficient $f$ in Eq. (1), by introducing a shape factor, $f_{nc}$, to account for the additional pressure loss caused by the non-circular and/or non-straight flow paths. For example, the present simulation study involved modeling two-phase flow in the annulus and through tubing
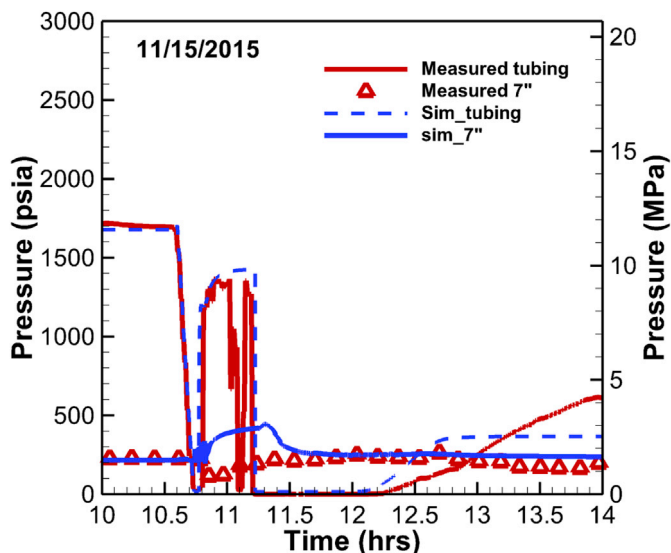
**Fig. 8.** Comparison of simulated tubing (blue dashed line) and casing (blue solid line) pressures against measured values during the 242 bbl kill. The sudden large drop in the measured tubing pressure in the middle of injection reflects the effects of the heavier (18 ppg) barite pill injection which we do not expect to see in the numerical model because we modeled only a single fluid with properties representative of a mixture of the kill-fluid compositions. (For interpretation of the references to colour in this figure legend, the reader is referred to the web version of this article.)

perforations and open sliding-sleeve valve ports (i.e., SSV slots) connecting the tubing with the A-annulus, and along flow paths that change direction from vertical to horizontal and vice versa. The shape factor is the square of the ratio between the diameter of a circular pipe, $D_c$, and the equivalent diameter, $D_{eq}$:

$$f_{nc} = \left(\frac{D_c}{D_{eq}}\right)^2 = \left(\frac{4A/\Gamma}{2\sqrt{A/\pi}}\right)^2 \tag{2}$$

For circular pipe(s), the shape factor will reduce to unity (i.e., value of 1) because $\Gamma = 2\pi\sqrt{A/\pi}$. For the annulus, the shape factor will be proportional to the difference between the inner radius of the casing and outer radius of the tubing wall.

The thermophysical properties and phase diagnostics are calculated using the equation of state model for real gases and brine implemented in EOS7Cma (Oldenburg and Pan, 2013b) which is a modification of EOS7C (Oldenburg et al., 2004). EOS7Cma has capability to simulate non-condensable gas components such as methane ($CH_4$) and air in addition to the brine. The kill fluid is simulated as brine with appropriately increased density and viscosity relative to pure water, whose density and viscosity are functions of pressure and temperature. All fluids are assumed to be Newtonian.

## 3. Model setup

### 3.1. Conceptual model

Fig. 1 shows a sketch of the SS-25 well derived from its record available from DOGGR (https://secure.conservation.ca.gov/WellRecord/037/03700776/03700776%20Data_03-19-08.pdf accessed July 20, 2017). The failure of the well is believed to have occurred because of a production casing integrity failure at a depth of ~134 m (440 ft) below the wellhead as evidenced by temperature logs which showed maximum cooling at this depth. Based on the magnitude of the flow, the casing failure was conjectured to be a gap or hole in the casing several cm (~1 inch) or more in size. Gas flows into the well from the
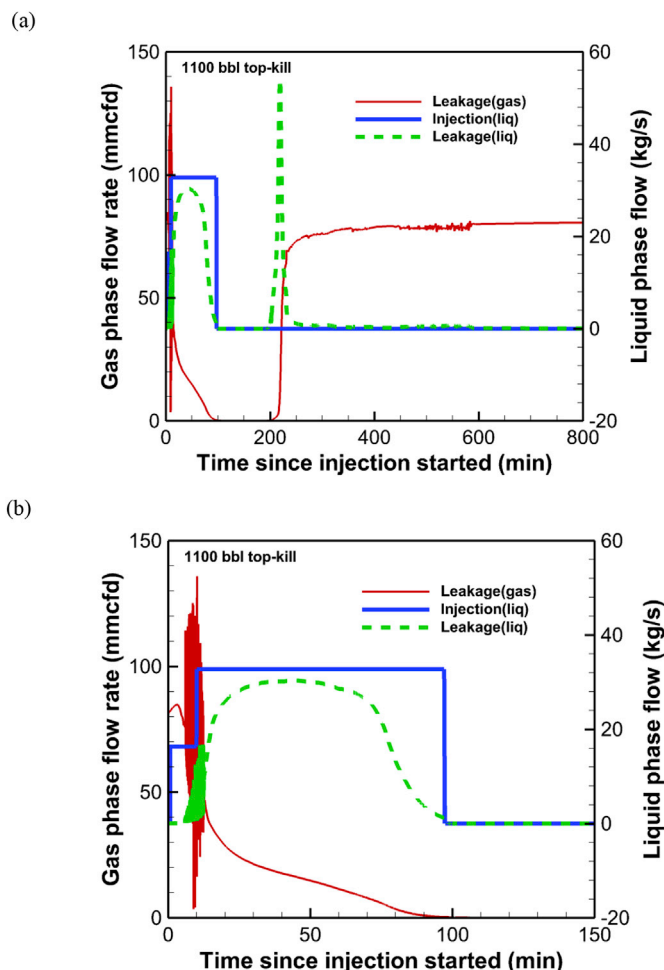




**Fig. 9.** Simulated gas (red thin line) and liquid (green dash line) leakage rate through the casing failure plotted along with the injection rate of kill fluid (blue solid line) for the 1100 bbl kill, (a) entire period, and (b) early time. (For interpretation of the references to colour in this figure legend, the reader is referred to the web version of this article.)

reservoir through the liner screen installed below 2617 m (8586 ft) and the production casing through perforations between 2594 and 2609 m (8510-8559 ft) (notional gas flow paths are shown as blue lines in Fig. 1). The gas then moves up into the tubing to the location where there was reportedly once an SSSV (subsurface safety valve). For unknown reasons, there are slots (open pathways) between the inner tubing and A-Annulus at this location, possibly indicative of later installation of a sliding sleeve valve (SSV). Regardless of how the tubing came to possess slots at this location, at the time of the SS-25 blowout in 2015 these slots provided a connection between the tubing and the A-annulus.

In the blowout scenario, gas flows up the A-annulus and then leaks through the casing failure at ~134 m (440 ft) below the wellhead and flows into the B-annulus. Although the B-annulus is cemented, a kink in the temperature logs suggests the gas flowed to the bottom, or nearly so, of the surface casing after exiting the production casing. The gas entered the geologic material around the well at this depth either through a breach near the base of the surface casing or through the opening at the bottom of the surface casing. Based on gas emanating from fractures in the ground surface down the slope to the west of the wellhead at the start of the blowout, it appears that due to its high pressure the gas fractured through the geologic material from where it exited the surface casing to the ground surface.

Because the tubing was plugged at a depth of 2559 m (8393 ft) (above the SSV slots) and perforated above the plug, the kill fluid injected down
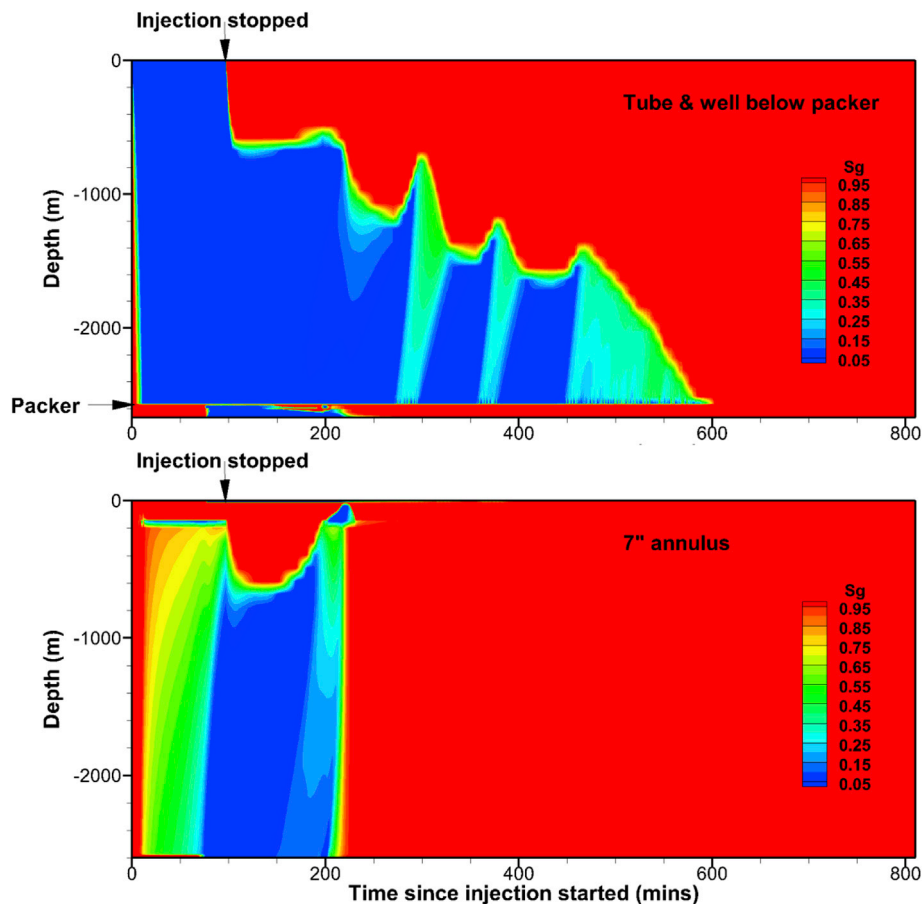
**Fig. 10.** Simulated gas saturation in the tubing and well below the packer (upper panel) and 7" (7-in) annulus (lower panel) during the 1100 bbl kill.

the tubing from the wellhead must flow through the perforations above the plug and then into the gas-filled and flowing A-annulus. In order to have a successful kill by this approach, kill fluid needs to build up in the A-annulus to create a high enough pressure to overcome the gas flow exiting the open SSV slots, or the combination of pressure and flow resistance (dynamic kill) needs to overcome the gas pressure at the SSV slots. Either way, kill fluid needs to accumulate significantly in the A-annulus and avoid being entrained by upward-flowing gas.

### 3.2. Radial grid

We developed a radially symmetric grid for T2Well to simulate the complex configuration in the well and its coupling to the surrounding reservoir, cap rock, and shallow formations (Fig. 2). The tubing wall is explicitly described in the grid as special grid cells from the top of the well down to the packer which separates the A-annulus from the tubing. Tubing walls are impermeable to the fluid (i.e., only conductive to heat flow) except at the tubing perforations and the open SSV slots. At the perforations, the tubing grid blocks and annulus grid blocks are directly connected with a total cross-sectional area corresponding to the area of 16 perforation holes. The total perimeter of the perforation holes is also assigned to that connection to accurately account in the T2Well flow calculations for the multi-hole geometry and its effects on flow resistance caused by the perforations. Similar approaches are used for the SSV slot connections; actual cross-sectional areas and perimeters of six SSV slots are summed to assign the correct area and perimeter for the connection. The production casing wall is modeled as impermeable with connections between the A-annulus cells and the surrounding formation cells allowing only for conductive heat flow. For the location where the production casing failed, an effective open area of $3.054 \times 10^{-3}$ m$^2$ (equivalent to a

2.46 in diameter hole) is used for that connection based on a calibration described below. The effective open area of the screen installed below 2617 m (8586 ft) is assumed to be 3% of the bulk surface area of the liner. The same ratio is used for the perforated zone between 2594 and 2609 m (8510-8559 ft).

The land surface temperature is set to 15 °C with geothermal gradient of 20 °C/km. The upper boundary is open to the atmosphere except for the tubing and annulus which are closed. The lower boundary is closed while the far-field radial boundary (at 500 m away from the well center) is assumed to have constant pressure and temperature.

The major properties of formations and wellbore sections used in the modeling are shown in Table 2 and Table 3, respectively.

With this grid and properties of the system, we modeled non-isothermal flow from the reservoir zone into and up the production casing as well as injection of kill fluid through the tubing.

### 4. Results

#### 4.1. Modeling calibrations and system status during gas leakage

Because of limited availability of information and parameter values for both the well and the formations, we did a preliminary manual calibration of the model against the measured tubing and 7" (7-in) casing pressure data before the November 15, 2015 top kill operation, when the reservoir pressure is assumed to be 19.31 MPa (2800 psi). The poorly constrained parameters that we calibrated are (1) the area of the casing failure (hole), and (2) permeability of the shallow formation (formation 1 through 3). Fig. 3 shows the comparison of the simulated and the measured pressure data following manual calibration. The gas leakage rate predicted by the calibrated model is about 19 kg/s, which is within
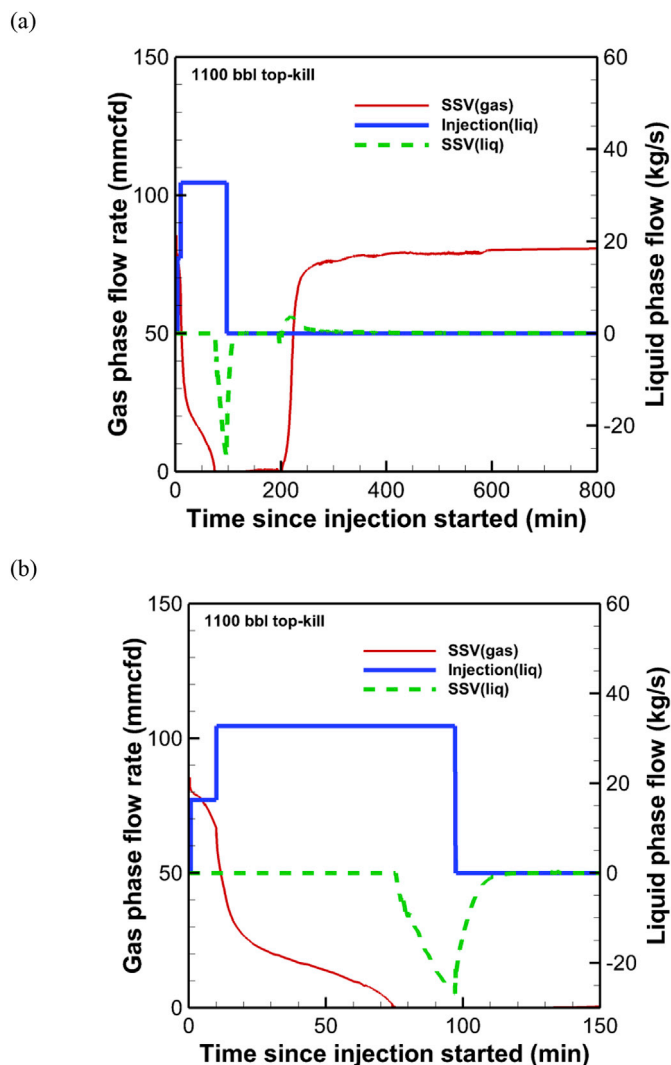
(a)



(b)



**Fig. 11.** Simulated gas (red line) and liquid (green dashed line) flow rates through the SSV slots from the tubing side to the annulus side as a response to the injection of kill fluid (blue line) during the 1 100 bbl kill. Negative values indicate flow from the annulus side to the tubing side through the SSV slots. (For interpretation of the references to colour in this figure legend, the reader is referred to the web version of this article.)

the range of the peak leakage rate measured by Scientific Aviation (Conley et al., 2016).

As shown on Table 4, the gas velocity varies greatly along the complex gas-flow pathway. The velocity increases significantly as the flowing gas enters the tubing (a narrow pathway). At the tubing below the open SSV slots (Point 3 in Fig. 4), the gas velocity is 70.24 m/s (~150 mph). This implies that the flowing gas carries large upward momentum at this location. An on-site engineer stated that a survey instrument lowered into the well behaved as if it hit a wall at that depth and the instrument broke immediately. After entering the annulus, the gas velocity decreases because of its relatively larger cross-sectional area compared to the tubing. By the point the gas reaches the hole in the production casing at shallow depth, the gas has become much less dense because of the lower pressure and velocities again become very large. Based on the gas velocity distribution pattern revealed here, it can be anticipated that the probability and flow rate of the kill fluid entering the A-annulus through the tubing perforations (Point 6), is larger than the probability and rate of the kill fluid entering the tubing through the open SSV slots (Point 4) against the more rapidly outflowing gas.

### 4.2. Two top-kill attempts

We simulated two of the seven top-kill attempts mainly because more information was available for these two than for the others. In the first kill attempt we simulated, 220 bbl of 9.4 ppg $CaCl_2$ solution and 22 bbl of 18 ppg barite pill were used in a 242 bbl kill attempt on Nov. 15, 2015. In the second kill attempt we simulated, 100 bbl of 9.4 ppg $CaCl_2$ solution and 1000 bbl of water was used in the 1 100 bbl kill attempt on Nov. 25, 2015. Because T2Well cannot simulate two types of kill (liquid) fluid simultaneously, we used one kill fluid with properties representative of the mixed fluid properties. The volume-weighted average density was assumed for the fluid. We estimated the viscosity of the kill fluid according to the concentration of $CaCl_2$ based on published viscosity data of $CaCl_2$ solution (OxyChem, Calcium Chloride: A Guide to Physical Properties, http://www.oxycalciumchloride.com/(accessed July 20, 2017)) and pure water at 15.6 °C (NIST Chemistry webbook, http://webbook.nist.gov/chemistry/fluid/(accessed July 20, 2017)). An estimated factor is used to multiply the viscosity data for a given $CaCl_2$ solution to account for the effects of the barite pill on the mixture. Table 5 summarizes the properties of the kill fluid and the injection schedules used in the simulations. The mass injection rates were estimated based on average density of kill fluids from the reported (or planned) volumetric injection rate data.

Results of T2Well simulations can be represented as time plots of gas flow (million standard cubic feet per day; mmcfd) and liquid flow (kg/s), the latter of two kinds: (i) into the well as kill fluid, and (ii) out of the well as kill-fluid return flow (kill fluid that returns to ground surface). Fluid or gas flows out of the ground surface are referred to as leakage.

As shown in Fig. 5, the gas leakage rate increases slightly immediately after the injection of kill fluid because the residual gas in the tubing is driven into the annulus and contributes to the gas leakage volume. Gas leakage then decreases, although not smoothly, as the kill fluid enters the annulus. Oscillations in fluid and gas flow become severe after the leaking gas starts to lift the injected kill fluid (green line) out of the A-annulus and into the overburden. The strong oscillations in both gas and liquid leakage rates are indicative of complicated phase interferences between the fast upward-flowing gas and the injected kill fluid in the annulus. This type of slugging behavior was likely the cause of observed oscillations of the well casing within the eroded cavities around the wellhead. Notably, when the kill-fluid injection rate increases, the amplitude of the oscillations in gas leakage rate gradually decreases and finally ceases so that the flows become smoothly varying and the gas leakage rate gradually decreases while the liquid leakage rate gradually increases.

Although the gas leakage rate decreases, it never reaches zero (the well is not killed). The simulation shows that a few minutes after the kill-fluid injection stops, the gas leakage rate recovers to its pre-kill level after having blown the kill fluid out of the A-annulus into the overburden and from there out of the subsurface entirely. The simulated kill failed because the liquid fraction of the two-phase mixture in the A-annulus was never high enough to create a column of fluid that imposed a back pressure at the SSV sufficient to stop the gas flow. Instead, the injected kill fluid was effectively carried out of the well with the gas under this limited injection intensity (up to 23.61 kg/s) and never entered the well below the packer through the open SSV slots (Fig. 6). As a result, the kill fluid never reached the well below the packer (Fig. 7, upper panel). The A-annulus becomes two-phase during the kill, but the liquid is swept out after the injection stops and it returns to being single-phase gas (Fig. 7, lower panel).

Measured and simulated tubing pressure responses roughly match, giving confidence in the model (Fig. 8). Because the kill fluid was modeled using "average" properties, the big pressure drop due to injection of the denser barite pill is not expected to be observed in the model results. In addition, because the perforations in the tubing are spread over a length of 3 m (9.8 ft) along the tubing (i.e., 16 holes at eight depths) whereas we simulated the perforations as a single effective hole,
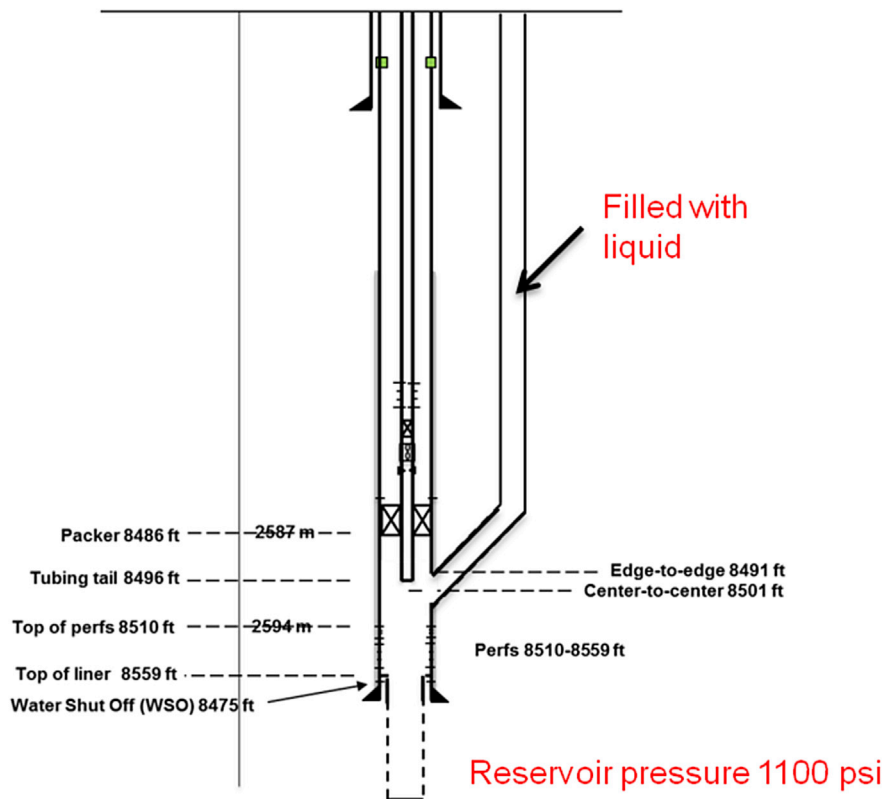
**Fig. 12.** Sketch of the SS-25 well intersected by the relief well (not to scale). The fluid in the relief well drains into the SS-25 well reservoir region below the packer immediately after the casing is milled through.

the gradual recovery trend of the tubing pressure due to sequential exposure of perforations to gas flow (gas flows into tubing through the top holes while water flows into the annulus through the bottom holes) cannot be reproduced by the model either. Poor match of the 7" (7-in) casing pressure during the injection period is because the leakage pathway through the shallow formations (including casing hole, the crater, and larger fractures in between) was approximated as porous

media in the model. Although the permeabilities were calibrated against the measured tubing and 7" (7-in) casing pressure data before the November 15, 2015 top kill operation, the parameters of the relative permeability functions were not calibrated. As a result, the model over-estimated the resistance to two-phase flow in that pathway.

The early response of the gas leakage rate to kill-fluid injection in the 1 100 bbl kill attempt is similar to the case of the 242 bbl kill (Fig. 9b), i.e., gas leakage increases slightly in the first 5 min because of the increased pressure of the kill-fluid injection. With higher injection rate (39% higher) and longer injection period (160% longer), however, the 1 100 bbl kill was able to reduce the gas leakage rate to zero after about 90 min, which was about 10 min before the end of the injection. The associated liquid leakage rate also becomes zero and the well "lays down" for about 100 min before gas leakage resumes and quickly recovers to its pre-kill level (Fig. 9a). The return to blow-out flow conditions occurs like the eruption of a geyser with strong oscillations in liquid flow through the casing failure.

The reason that the blowout flow "lays down" is because the liquid column in the annulus becomes high enough (Fig. 10, lower panel) after about 75 min of injection to stop the gas flow through the SSV slots and the resulting pressure causes liquid to flow into the tubing below the plug. (Fig. 10, upper panel, and Fig. 11). As a result, kill fluid fills the well below the packer (Fig. 10, upper panel). However, when injection of the kill fluid ceases, the buildup of liquid in the annulus ceases. The pressure in the annulus at the SSV slots is still high enough to cause liquid to flow through the slots into the tubing (Fig. 11B) to replenish fluid below the packer that is entering the reservoir, but this decreases average liquid saturation in the annulus as kill fluid is depleted from the tubing (Fig. 10, upper panel). This causes the pressure in the annulus at the SSV slots to decrease until it is no longer large enough to cause liquid to flow into the tubing through the slots at about 13 min after the cessation of kill fluid injection (Fig. 11B). However, the liquid below the packer is still draining into the reservoir, allowing a gas "bubble to form below the packer
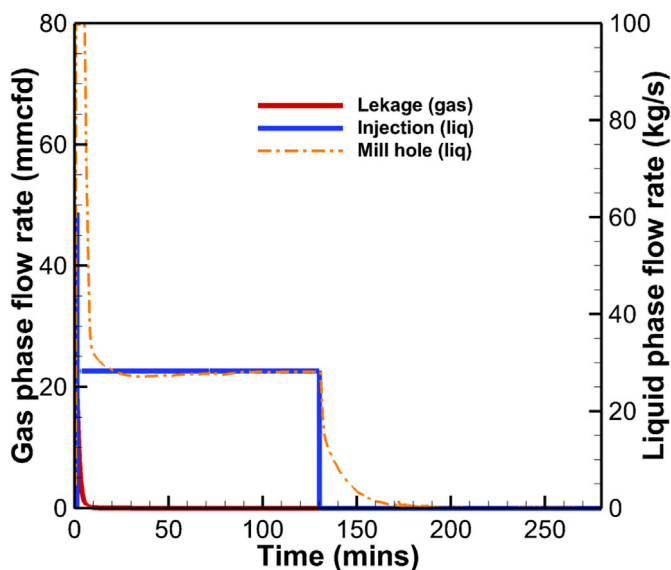


**Fig. 13.** Simulated gas leakage rate (red solid line), relief-well fluid injection rate (blue solid line), and liquid flow rate through the mill hole (red dash-dot line) from the relief well to the SS-25 well during the relief-well kill attempt. The injected liquid (blue line) is 9.0 ppg CaCl$_2$ solution. (For interpretation of the references to colour in this figure legend, the reader is referred to the web version of this article.)
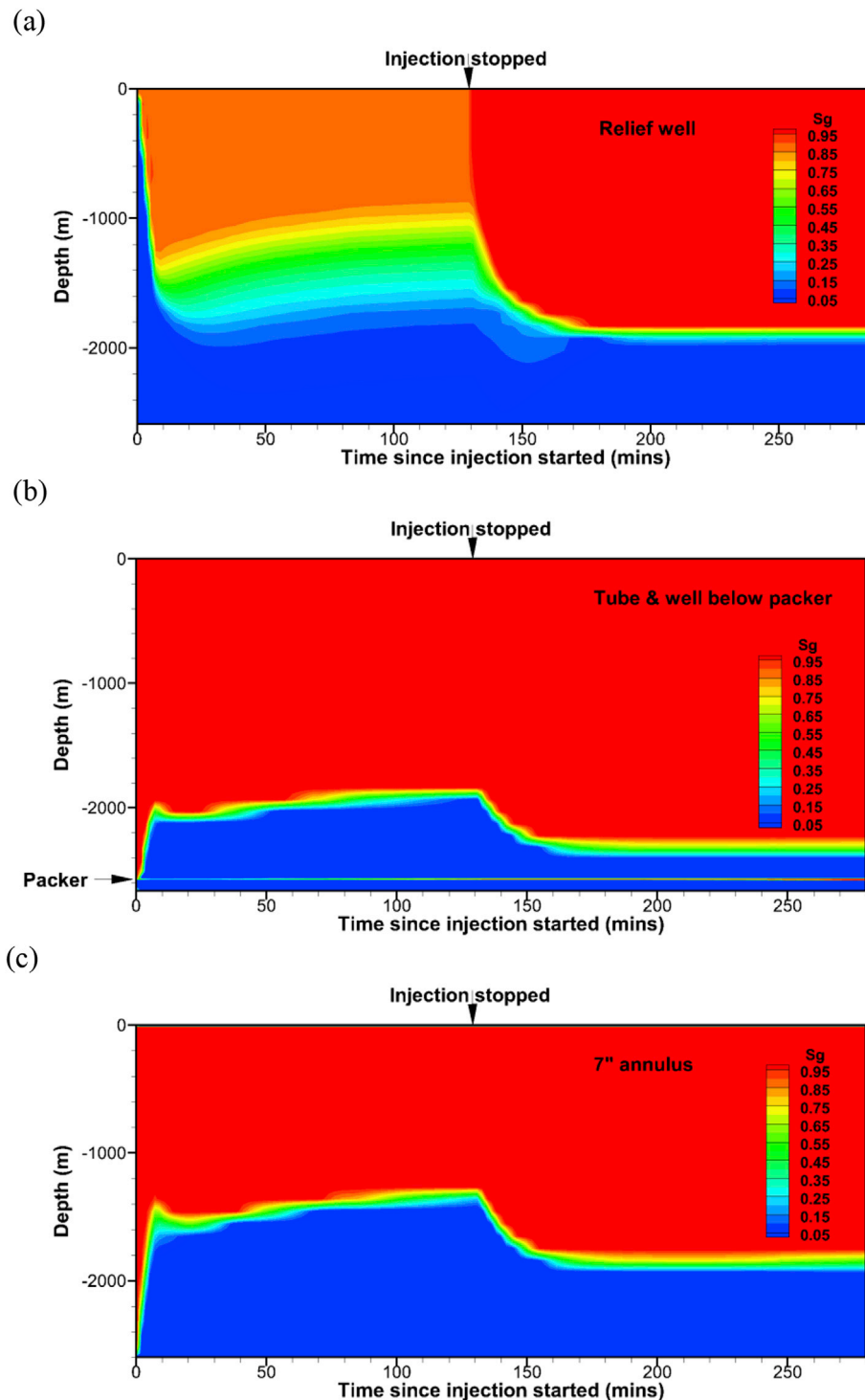
(a)



(b)

(c)

**Fig. 14.** Simulated gas saturation during relief-well kill in (a) the relief well over time, (b), tubing and well below the packer, and (c), 7" (7-in) annulus.

(Fig. 10, upper panel). About 50 min after the cessation of injection (150 min after the start), the gas "bubble" becomes tall enough to develop more pressure in the tubing at the SSV slots than the liquid in the annulus is imposing, and gas starts to enter the annulus again (Fig. 10 lower panel, and 11A). The depth to the top of the liquid column decreases as it expands due to the gas inflow (Fig. 10, lower panel). About 100 min after the end of injection and 200 min after the start of injection, the top of the liquid column reaches the production casing breach and liquid starts to exit the production casing (Fig. 10, lower panel, and 9A). The liquid in the annulus is quickly carried out of the well with the

flowing gas in the form of a geyser like eruption (Fig. 9A). The resulting decrease of pressure in the well below the packer causes some of the kill fluid that has entered the reservoir to flow back into the well and also be ejected through the SSV slots (Fig. 10, upper panel, and 11A).

### 4.3. Kill with relief well

In this simulation, we added the relief well to the coupled wellbore-reservoir model described above as an additional one-dimensional domain connected to the SS-25 domain in the reservoir (Fig. 12). As in
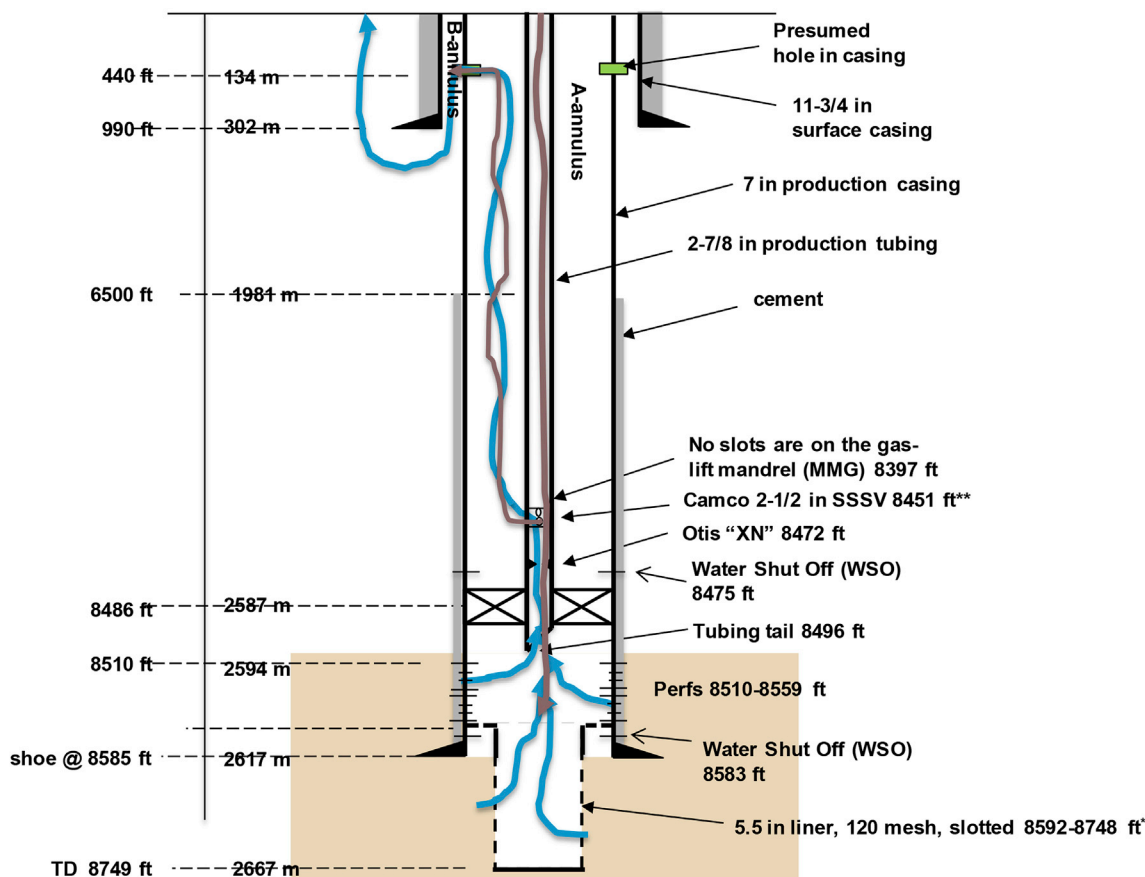
**Fig. 15.** A sketch of the SS-25 well without the tubing plug and perforations (not to scale) and possible flow upward flow path of gas leakage (blue) and downward flow of kill fluid (brown). In this hypothetical configuration, the kill fluid (brown) can flow down directly to the well below the packer although a fraction may be carried away by the leaking gas through the SSSV slots. See Fig. 1 for explanation of components.

the actual system just prior to successful killing of the SS-25 blowout, the relief well is connected to the SS-25 well through a hole that was created by milling through the casing of the SS-25 well. All other model parameters and boundary conditions are the same as presented in Section 4.2 except that the initial conditions in the SS-25 well and the formations were calculated assuming the reservoir pressure had decreased to 1 100 psi. We make this assumption because approximately 100 days of leakage and gas drawdown by production (through other wells) was carried out before the relief-well kill in February 2016. The relief well is initially filled with drilling fluid (9.0 ppg CaCl₂ solution) at hydrostatic pressure and is under continuous injection with the same fluid (1 100 bbl). The mass flow rate in the T2Well model through the mill hole is limited to 100 kg/s for numerical stability.

As shown in Fig. 13, gas leakage at the surface stops within 10 min after milling into SS-25, which is consistent with the field observations. The effectiveness of the relief-well kill is due to the large liquid inflow through the mill hole below the packer (Fig. 12). The large amount of the liquid in the relief well almost immediately fills the critical portion of SS-25 (i.e., the well below the packer) exerting pressure on the reservoir and stopping gas flow into the well (Fig. 14). The liquid then "U-tubes" up the SS-25 well tubing, out the SSV slots and into the lower portion of the annulus. The liquid even flows back into the tubing through the tubing perforations above the plug as the liquid level further increases in the annulus. After the injection stops, the liquid levels in the relief well and the annulus tend to approach the same height as they form a U-tube configuration (Fig. 14a and c). The lower liquid level in the tubing is caused by the pressurization of the gas bubble trapped in the top portion of the tubing (Fig. 14b). There are two other compressed gas bubbles, one in the dead end of the tubing above the SSV and below the plug in the tubing and the other in the dead end of the production casing around the

tubing below the packer (Fig. 14b), but these gas bubbles have little effect on stopping gas leakage from the reservoir because of the large pressure exerted by the liquid filling the wells in the U-tube configuration. We note these compressed gas features of our simulations did not play a critical role in the success of the relief-well kill, but they could inhibit fluid entry and are potentially important aspects of the flow system which our T2Well model faithfully simulated.

Presumably the well blowout would eventually restart some time after cessation of injection via the relief-well kill due to fluid loss to the reservoir, just as it did after the two top kills simulated. However in practice SS-25 was plugged with cement via the relief well within a day of the kill.

## 5. Discussion

### 5.1. Effects of the configuration of tubing plug and perforations

To investigate the possible effects of the tubing plug and perforations on the top kill, we simulated a hypothetical scenario of 1100 bbl kill attempt on the well assuming there was no tubing plug nor associated perforations (Fig. 15). Based on the few details available regarding the top kill attempts prior to setting the plug in and perforating the tubing, this hypothetical "no plug" case was designed to use more kill fluid in order to provide a limiting case.

With no plug in the tubing, the injected kill fluid does not need to enter the annulus through tubing perforation holes before re-entering the tubing by overcoming the pressure of the gas flowing from the SSV slots into the annulus. Instead, the kill fluid can flow down directly to the well below the packer through the tubing, although a fraction may be carried away by the leaking gas through the SSV slots. All other parameters are
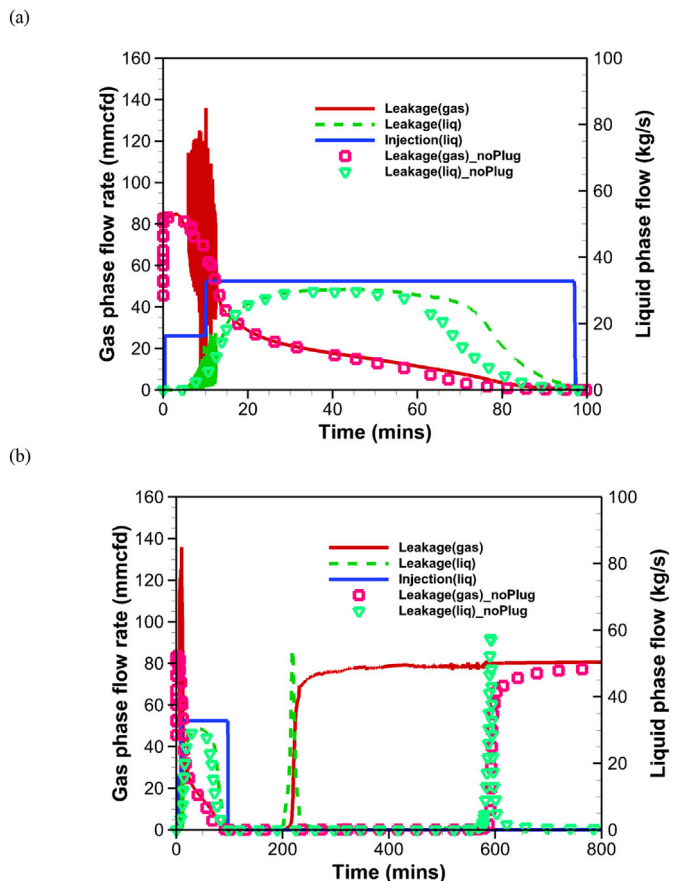
(a)



(b)



**Fig. 16.** Comparison of simulated flow rates in response to the same 1100 bbl kill attempt for the base case (tubing plug and perforations) and the hypothetical no-plug case (no tubing plug and perforations) for (a) the first 100 min, (b) the entire simulated period.

(a)



(b)



**Fig. 17.** Comparison of simulated flow rates through the SSV slots in response to the same 1100 bbl kill attempt for (a) the first 100 min, and (b) the entire simulated period. The "noPlug" case contains no tubing plug nor perforations. Flow from the tubing side to the annulus side through the SSV is positive. We plot the injection of kill liquid (blue) for reference. (For interpretation of the references to colour in this figure legend, the reader is referred to the web version of this article.)

the same as those of the 1100 bbl kill attempt described in Section 4.2.

The simulated gas leakage in response to the injection of kill fluid for the base-case (tubing plug and perforations) and no plug case are shown for comparison in Fig. 16. The gas leakage response is almost the same at early time (Fig. 16A) for both cases except that the strong oscillations in gas and liquid leakage rates do not occur in the no plug case. When the gas leakage rate decreases to a certain rate, the liquid leakage rate starts to decrease because of the diminishing gas lift. However, this phenomenon takes place slightly earlier in the no plug case. On the other hand, in both cases, the gas leakage ultimately recovers to its pre-kill level following an eruption of liquid after the well is temporarily "dead" (Fig. 16B). However, without the tubing plug and perforations structure the length of the "lay-down" period increases from about 100 min to 500 min (Fig. 16B). In other words, the tubing plug and perforations increase the difficulty of controlling pressure in the SS-25, thereby preventing effective top kills of the well. But we emphasize that in both cases, the gas leakage resumes eventually if the injection of kill fluid is stopped due to loss of this fluid to the reservoir. These simulations are consistent with the experience that fluid levels need to be maintained in wells to maintain pressure control once the high flow-rate gas release has been stopped, for instance during workovers.

Looking the simulated flows through the SSV slots in the no plug case, we see that at early time almost all of the injected liquid is carried away by the leaking gas flow through the SSV slots into the annulus (green triangles, Fig. 17A) while no liquid could enter the tubing side of the SSV slots from the annulus in the base case. When the gas leakage rate drops significantly and approaches zero, the liquid starts to flow down into the well below the packer so that the trend of liquid flow rate through the
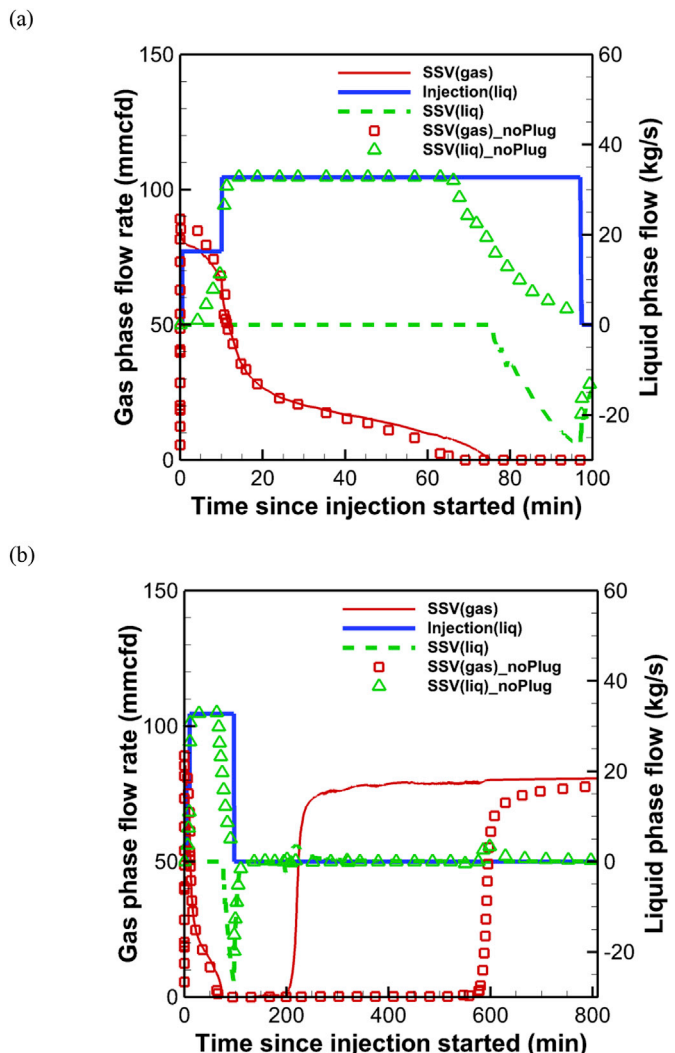
SSV starts to deviate from the injection curve in the no plug case (Fig. 17A). In the base case, about 10 min later, liquid starts to enter the tubing side of the SSV from the annulus (green dashed line, Fig. 17A). After liquid breaks through the gas-flow barrier, the rate of liquid flow into the bottom of the well increases with time in both cases until the end of the injection. Only a small amount of liquid flow from the tubing out to the annulus is associated with the resumption of gas leakage in both cases (Fig. 17B). This implies that the liquid forming the eruption at the start of resumption of gas leakage is primarily derived from the liquid sitting in the annulus.

Fig. 18 shows the gas-saturation profiles in the tubing (including in the well below the packer) and annulus over time. Unlike in the default case, where there still is a large amount of liquid trapped in the tubing when the gas leakage resumes (Fig. 10), removing the tubing plug effectively eliminates the occurrence of liquid that was trapped in the tubing and unable to enter the leakage flow path (i.e., A-annulus) through the perforations (Fig. 18). The process of decreasing liquid saturation in the annulus (i.e., the preparation of resumption of gas leakage) is much longer in the no plug case (Fig. 18) than the default case
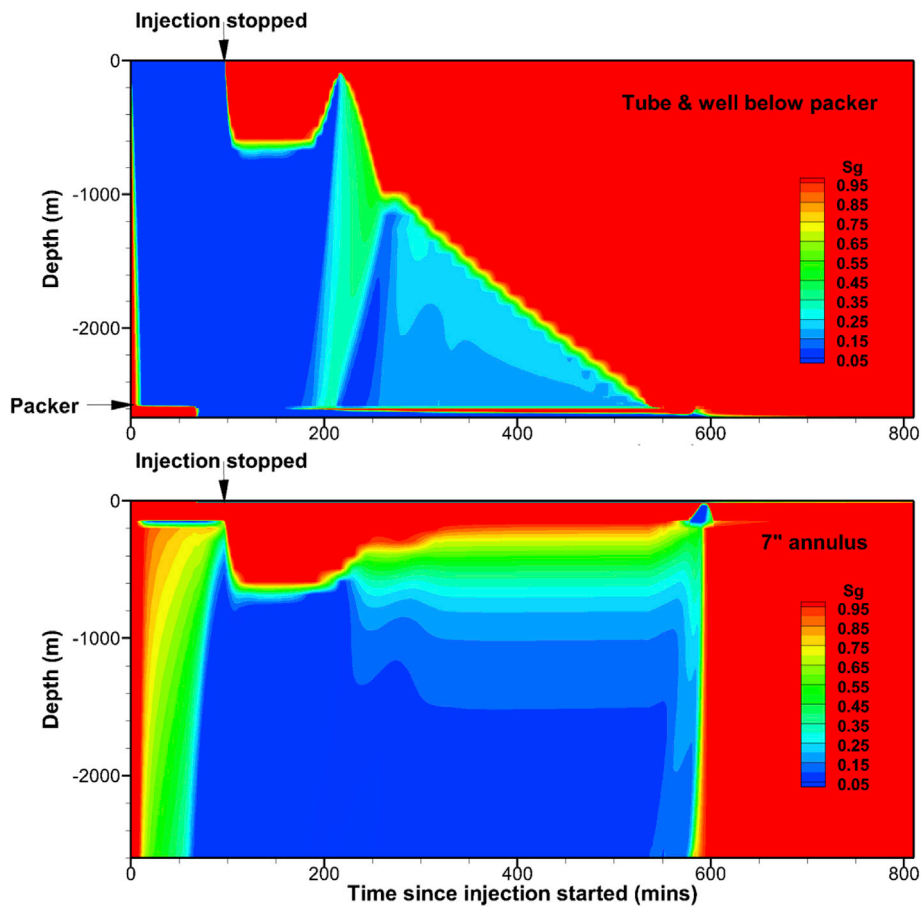
**Fig. 18.** Simulated gas saturation in tubing and in well below the packer (upper panel) and 7″ annulus (lower panel) during the 1100 bbl kill without the tubing plug or perforations.
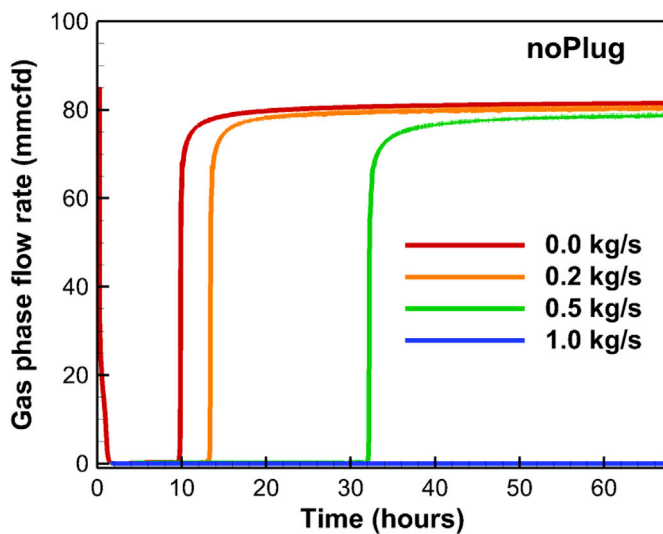


**Fig. 19.** Simulated gas leakage rate in response to different follow-up injection rates after the 1 100 bbl kill attempt for no-plug case. The default (red line) is the case where no follow-up liquid injection occurs after the main 1 100 bbl injection. (For interpretation of the references to colour in this figure legend, the reader is referred to the web version of this article.)

(Fig. 10) because all of the liquid in the tubing has to be drained first in the no plug case. In other words, we have more liquid built up to halt gas leakage in the no plug case than in the base case for the same amount of injection. This is the reason that the leaking well "lays down" for a much

longer time in the no plug case than in the base case.

### 5.2. Test of alternate approach for top kill of SS-25

As suggested by the simulation results of the no plug case, it appears that one could "lay down" the leaking well longer if the well below the packer and the annulus remained fluid-filled for a longer time. The idea here is that the SS-25 well with its complex geometry, and any other well with simpler conditions (e.g., analogous to our no plug case), could perhaps be killed successfully by continuous fluid injection rather than having to resort to the slow and costly drilling of a relief well. In order to test alternate kill approaches, we carried out a set of numerical simulations with various follow-up injection rates that could be prescribed after the initial 1 100 bbl are injected for the top kill.

The model set up and parameters are the same as the no plug case, chosen because it is potentially more representative of typical wells rather than the SS-25, which ended up with a plug and perforations following initial mitigation efforts. Fig. 19 shows the gas leakage rates in response to the different follow-up injection rates. As expected, the larger the injection rate, the longer the "lay down" condition will last. If the follow-up injection is at a rate of 1 kg/s, the well is practically "dead." This is directly related to the duration of fluid-filled annulus (Fig. 20). For injection rates larger than 1 kg/s, the liquid column in the annulus quickly reaches a stable condition which blocks the leakage of gas. For other cases, the liquid saturation will gradually decrease for a relatively short period before sudden expulsion of liquid by the resumed gas flow. These gradually decreasing periods often start when the liquid column in the tubing almost disappears (Fig. 21). Therefore, keeping a certain height of the liquid column in the tubing is critical to keeping the well "dead." The minimum follow-up injection rate should be between 0.5 kg/
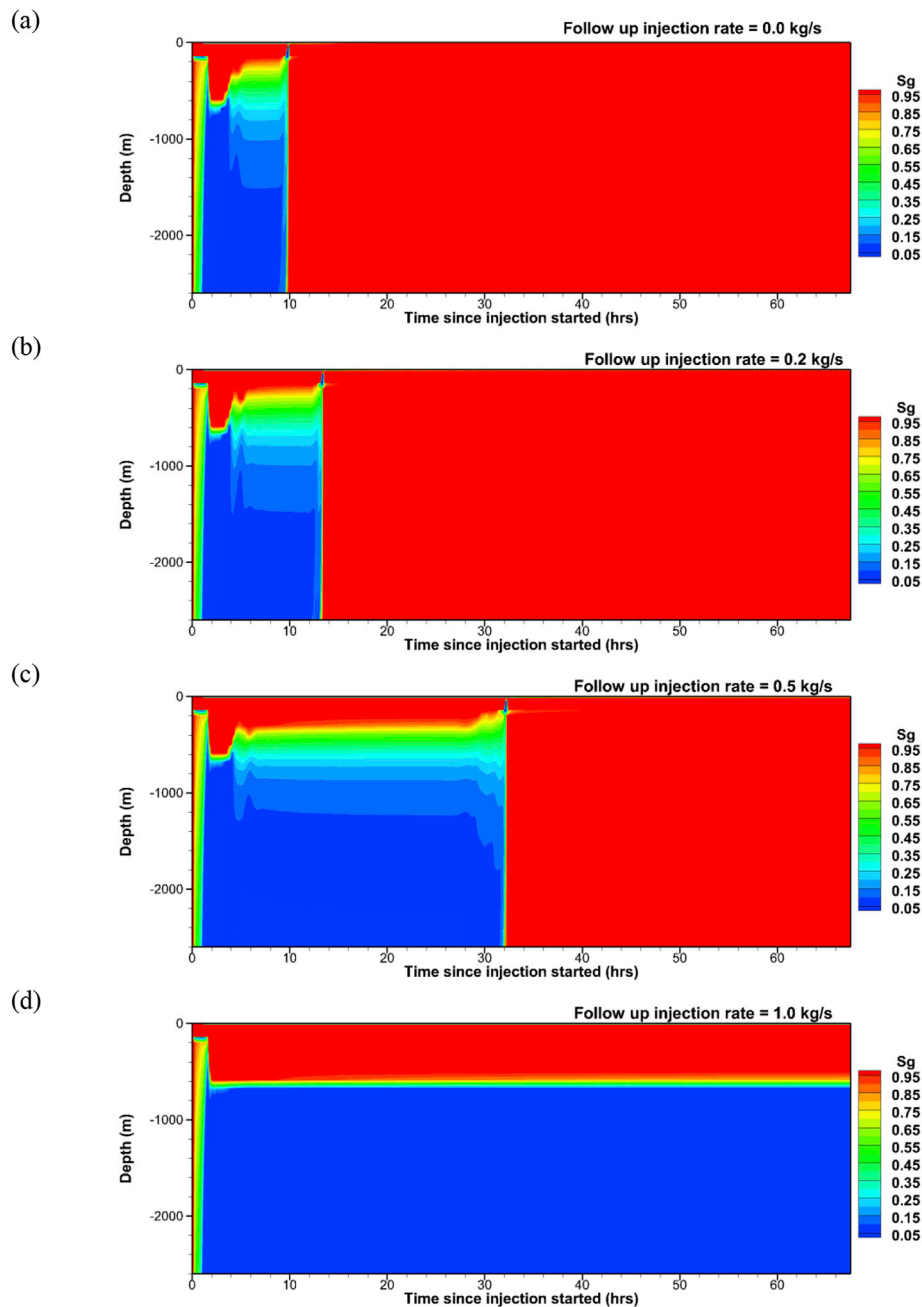
(a)



(b)



(c)



(d)



**Fig. 20.** Simulated evolution of gas saturation in the 7″ annulus in response to different follow-up injection rates after the main 1100 bbl kill attempt for the system without the tubing plug).

s and 1.0 kg/s for the modeled system. Interestingly, a gas bubble develops first in the well below the packer about 2 h after the sudden drop in injection rate in all cases (Fig. 21). However, this gas bubble is kept in check in the 1 kg/s followup injection case because maintenance of the liquid column height sustains the necessary backpressure on the bubble.

## 6. Conclusions

During early efforts to control SS-25, a plug was installed in the well tubing and the tubing was subsequently perforated above the plug to regain access to the well. These openings along with the open SSV slots in the tubing created a complex flow path for gas and kill fluid between the tubing and A-annulus. Simulations of flowing gas and top-kill and relief-well kill processes have been carried out using T2Well, a coupled well-reservoir simulator based on the TOUGH codes. T2Well uses

compressible Navier-Stocks momentum equation (with the drift-flux model) to simulate flow in the well and couples the well region with porous media regions in which flow is governed by Darcy's law. Using detailed properties of the well and the calibrated and known parameters, T2Well simulations match observed pressures and provide plausible temperatures for flowing gas.

Our simulation results capture complex two-phase flow and geometry-related aspects of the system and provide a basis for understanding the top-kill failures, behavior of the relief-well kill, and the effectiveness of hypothetical scenarios for the SS-25 well. The SSV resulted in a substantial portion of the top-kill fluid being ejected from the breach in the SS-25 production casing breach as compared to conventional well configurations with no such connection between the tubing and A-annulus. As a result, many times more kill fluid was required than a simple calculation of the well volume would indicate,
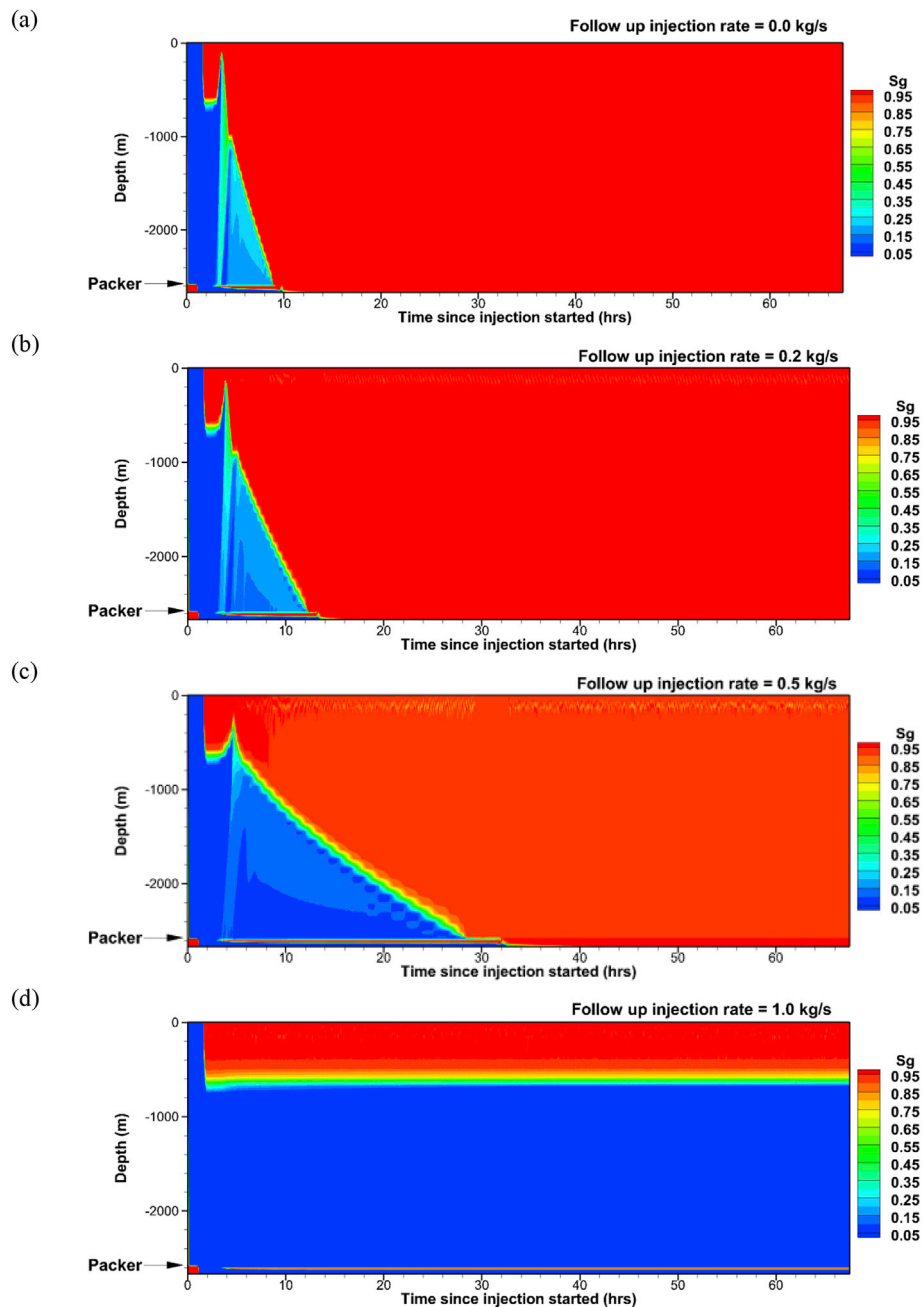
(a)



(b)

(c)

(d)

**Fig. 21.** Simulated evolution of gas saturation in the tubing and well below the packer in response to different follow-up injection rates after the main 1100 bbl kill attempt for the system without the tubing plug.

which is the sufficient volume for conventionally configured well. In the cases of sufficient kill fluid volume and rate to stop the gas flow temporarily, the tubing plug-perforation combination shortened the cessation of gas flow substantially because the resumption of gas flow trapped fluid in the tubing. With no plug in the tubing, the liquid column in the tubing retards the gas flow through the SSV, lengthening the time until this gas has expanded the liquid in the A-annulus up to the production casing breach. Finally, the leakage of kill fluid into the reservoir without a compensatory continued injection of kill fluid caused SS-25 to resume blowing out.

The cumulative effect of these three factors appears not to have been discerned during the blowout as evidenced by the failure of the numerous top kills to stop the gas flow permanently, and the erosion ("cratering") around the casing below the well head resulting from these numerous kills necessitated commencing two relief wells (the second relief well was

started as a backup in case the first failed to stop the blowout for some reason). Consequently the failure to account for the cumulative impact of these factors extended the blowout period and increased the cost of bringing it under control.

This study demonstrates the value of a simulator capable of exploring multiphase fluid flow in complex well configurations coupled to a reservoir as compared to simpler straight pipe simulators. Although we started these simulation studies while the unsuccessful top kills were being carried out and worked extended hours to generate model results, we could not generate results that we were confident in fast enough to keep pace with the needs of the operator. This experience points out that reacting to incidents like the SS-25 blowout is problematic because it is difficult to keep pace with the crisis. Instead, it is imperative that operators develop the capacity to carry out simulations, or mine existing databases of pre-computed results, very quickly in response to incidents

such as the SS-25 blowout so that decision-making and responses can be made in a timely manner.

### Nomenclature

| | |
|---|---|
| $A$ | wellbore cross-sectional area $m^2$ |
| $b$ | formation thickness m |
| $C_0$ | shape factor |
| $\mathbf{g}$ | acceleration of gravity vector $m\ s^{-2}$ |
| $E$ | Energy J |
| $\mathbf{F}$ | Darcy flux vector $kg\ m^2\ s^{-1}$ |
| $H$ | enthalpy J |
| $h$ | specific enthalpy $J\ kg^{-1}$ |
| $k$ | permeability $m^2$ |
| $k$ | relative permeability |
| $m$ | mass kg |
| $\mathbf{n}$ | outward unit normal vector |
| $p$ | total pressure Pa |
| $Q$ | heat J |
| $q_v$ | volumetric source term $kg\ m^{-3}\ s^{-1}$ |
| $R$ | radial coordinate, gas constant $m,\ J\ kg^{-1}\ mol^{-1}$ |
| $S$ | saturation, storativity $-,\ m^{-1}$ |
| $t$ | time s |
| $T$ | temperature, transmissivity $^\circ C,\ m\ s^{-1}$ |
| $u$ | *Darcy* velocity of phase $\beta$ $m\ s^{-1}$ |
| $uG,\ uL$ | *phase velocity of gas and liquid in the well* $m\ s^{-1}$ |
| $U$ | internal energy $J\ kg^{-1}$ |
| $v$ | velocity $m\ s^{-1}$ |
| $V$ | volume $m^3$ |
| $W$ | work J |
| $X$ | mass fraction w/phase subscript and component superscript |
| z | *Z*-coordinate (positive upward) m |
| $Z$ | compressibility factor |

*Greek symbols*

| | |
|---|---|
| $\alpha$ | fluid compressibility $Pa^{-1}$ |
| $\beta$ | phase index |
| $\beta_f$ | formation compressibility $Pa^{-1}$ |
| $\Gamma$ | surface area $m^2$ |
| $\theta$ | angle between wellbore and the vertical $^\circ$ |
| $\kappa$ | mass components (superscript) |
| $\lambda$ | thermal conductivity of fluid-rock composite $J\ m^{-1}\ s^{-1}\ K^{-1}$ |
| $\mu$ | dynamic viscosity $kg\ m^{-1}\ s^{-1}$ |
| $\rho$ | density $kg\ m^{-3}$ |
| $\tau$ | tortuosity |
| $\phi$ | porosity |

*Subscripts and superscripts*

| | |
|---|---|
| $\beta$ | phase index |
| cap | capillary |
| d | drift |
| G | gas |
| $\kappa$ | component index |
| l | liquid |
| lr | liquid residual |
| L | liquid |
| m | mixture |
| NK1 | energy component |
| 0 | reference value |

*r*        relative
*res*      bulk reservoir

## References

Bendiksen, K.H., Maines, D., Moe, R., Nuland, S., 1991. The dynamic two-fluid model OLGA: theory and application. SPE Prod. Eng. 6 (02), 171–180.

California Air Resources Board, 2016. Determination of Total Methane Emissions from the Aliso Canyon Natural Gas Leak Incident. Available at. https://www.arb.ca.gov/research/aliso_canyon/aliso_canyon_methane_emissions-arb_final.pdf.

Conley, S., Franco, G., Faloona, I., Blake, D.R., Peischl, J., Ryerson, T.B., 2016. Methane emissions from the 2015 Aliso Canyon blowout in los angeles, ca. Science 351 (6279), 1317–1320.

Dhulesia, H., Lopez, D., 1996. January. Critical evaluation of mechanistic two-phase flow pipeline and well simulation models. In: SPE Annual Technical Conference and Exhibition. Society of Petroleum Engineers.

Guo, C., Pan, L., Zhang, K., Oldenburg, C.M., Li, C., Li, Y., 2016. Comparison of compressed air energy storage process in aquifers and caverns based on the Huntorf CAES plant. Appl. ENERGY 181, 342–356.

Oldenburg, C.M., Moridis, G.J., Spycher, N., Pruess, K., March 2004. EOS7C Version 1.0: TOUGH2 Module for Carbon Dioxide or Nitrogen in Natural Gas (Methane) Reservoirs. Lawrence Berkeley National Laboratory Report LBNL-56589.

Oldenburg, C.M., Freifeld, B.M., Pruess, K., Pan, L., Finsterle, S., Moridis, G.J., 2012. Numerical simulations of the Macondo well blowout reveal strong control of oil flow by reservoir permeability and exsolution of gas. Proc. Natl. Acad. Sci. 109 50, 20254–20259.

Oldenburg, Curtis M., Pan, Lehua, 2013a. Utilization of CO2 as cushion gas for porous media compressed air energy storage. Greenh. Gas. Sci. Technol. 3, 1–12.

Oldenburg, C.M., Pan, L., 2013b. Porous media compressed-air energy storage (PM-CAES): theory and simulation of the coupled wellbore–reservoir system. Transp. Porous Media 97 (2), 201–221.

Pan, L., Freifeld, B., Doughty, C., Zakem, S., Sheu, M., Cutright, B., Terrall, T., 2015. Fully coupled wellbore-reservoir modeling of geothermal heat extraction using CO2 as the working fluid. Geothermics 53, 100–113.

Pan, L., Oldenburg, C.M., 2014. T2Well—an integrated wellbore–reservoir simulator. Comput. Geosciences 65, 46–55.

Pan, L., Webb, S.W., Oldenburg, C.M., 2011a. Analytical solution for two-phase flow in a wellbore using the drift-flux model. Adv. Water Resour. 34, 1656–1665.

Pan, L., Oldenburg, C.M., Wu, Y.-S., Pruess, K., 2011b. Transient CO2 leakage and injection in wellbore-reservoir systems for geologic carbon sequestration. Greenh. Gases Sci. Tech. 1 (4), 335–350.

Pan, L., Wu, Y.-S., Oldenburg, C.M., Pruess, K., 2011c. T2Well/ECO2N Version 1.0: Multiphase and Non-isothermal Model for Coupled Wellbore-reservoir Flow of Carbon Dioxide and Variable Salinity Water. LBNL-4291E.

Pruess, K., Oldenburg, C.M., Moridis, G.J., 1999. TOUGH2 User's Guide Version 2. E. O. Lawrence Berkeley National Laboratory Report LBNL-43134. LBNL-43134 (revised), 2012.

Ravndal, M., 2011. Models for Dynamic Kill of Blowouts. Master's thesis. University of Stavanger, Norway.

Rygg, O.B., Smestad, P., Wright, J.W., 1992. Dynamic two-phase flow simulator: a powerful tool for blowout and relief well kill analysis. January. In: SPE Annual Technical Conference and Exhibition. Society of Petroleum Engineers.

Shi, H., Holmes, J.A., Durlofsky, L.J., Aziz, K., Diaz, L.R., Alkaya, B., Oddie, G., 2005. Drift-flux modeling of two-phase flow in wellbores. Soc. Pet. Eng. J. 10 (1), 24–33.

Vasini, E.M., 2016. Numerical Modelling and Simulation Optimization of Geothermal Reservoirs Using the Tough2 Family of Codes (Doctoral dissertation, alma).